




3-O-Methyl-Alkylgallates Inhibit Fatty Acid Desaturation in *Mycobacterium tuberculosis*

Nidja Rehberg,^a Edwin Omeje,^a Sherif S. Ebada,^{a,b} Lasse van Geelen,^a Zhen Liu,^a Parichat Sureechatchayan,^c Matthias U. Kassack,^c Thomas R. Ioerger,^d Peter Proksch,^a  Rainer Kalscheuer^a

^aInstitute of Pharmaceutical Biology and Biotechnology, Heinrich Heine University Düsseldorf, Düsseldorf, Germany

^bDepartment of Pharmacognosy, Faculty of Pharmacy, Ain-Shams University, Cairo, Egypt

^cInstitute of Pharmaceutical and Medicinal Chemistry, Heinrich Heine University Düsseldorf, Düsseldorf, Germany

^dDepartment of Computer Science, Texas A&M University, College Station, Texas, USA

ABSTRACT In the quest for new antibacterial lead structures, activity screening against *Mycobacterium tuberculosis* identified antitubercular effects of gallic acid derivatives isolated from the Nigerian mistletoe *Loranthus micranthus*. Structure-activity relationship studies indicated that 3-O-methyl-alkylgallates comprising aliphatic ester chains with four to eight carbon atoms showed the strongest growth inhibition *in vitro* against *M. tuberculosis*, with a MIC of 6.25 μ M. Furthermore, the most active compounds (3-O-methyl-butyl-, 3-O-methyl-hexylgallate, and 3-O-methyl-octylgallate) were devoid of cytotoxicity against various human cell lines. Furthermore, 3-O-methyl-butylgallate showed favorable absorption, distribution, metabolism, and excretion (ADME) criteria, with a P_{app} of 6.2×10^{-6} cm/s, and it did not inhibit P-glycoprotein (P-gp), CYP1A2, CYP2B6 or CYP3A4. Whole-genome sequencing of spontaneous resistant mutants indicated that the compounds target the stearyl-coenzyme A (stearyl-CoA) delta-9 desaturase DesA3 and thereby inhibit oleic acid synthesis. Supplementation assays demonstrated that oleic acid addition to the culture medium antagonizes the inhibitory properties of gallic acid derivatives and that sodium salts of saturated palmitic and stearic acid did not show compensatory effects. The moderate bactericidal effect of 3-O-methyl-butylgallate in monotherapy was synergistically enhanced in combination treatment with isoniazid, leading to sterilization in liquid culture.

KEYWORDS 3-O-methyl-alkylgallate, DesA3, *Loranthus micranthus*, *Mycobacterium tuberculosis*, antitubercular, fatty acid desaturation, gallic acid, natural product, oleic acid

Tuberculosis (TB), caused by *Mycobacterium tuberculosis*, is the leading cause of death by an infectious disease (1). A total of 10.4 million people were newly infected by *M. tuberculosis* in 2016, and 1.7 million patients died of TB worldwide. The main areas of endemicity are located in sub-Saharan Africa and Southeast Asia. Frequent HIV coinfection, poverty, and decades of neglect in drug development complicate the containment of the disease. For more than 50 years, the standard therapy of TB has consisted of a 6-month drug regimen employing the four drugs isoniazid (INH), rifampin (RIF), ethambutol (EMB), and pyrazinamide (PZA). Although combination treatment reduces the likelihood of resistance development, multidrug-resistant (MDR) and even extensively drug-resistant (XDR) strains have evolved over the years and are seriously complicating control of the TB pandemic (2). MDR strains, which are resistant to RIF and INH, and XDR strains, which are additionally resistant to any fluoroquinolone and to one of the three injectable drugs capreomycin, amikacin, and kanamycin, represent a great burden for the health care sector due to prolonged therapy durations

Citation Rehberg N, Omeje E, Ebada SS, van Geelen L, Liu Z, Sureechatchayan P, Kassack MU, Ioerger TR, Proksch P, Kalscheuer R. 2019. 3-O-Methyl-alkylgallates inhibit fatty acid desaturation in *Mycobacterium tuberculosis*. *Antimicrob Agents Chemother* 63:e00136-19. <https://doi.org/10.1128/AAC.00136-19>.

Copyright © 2019 American Society for Microbiology. All Rights Reserved.

Address correspondence to Peter Proksch, proksch@hhu.de, or Rainer Kalscheuer, rainer.kalscheuer@hhu.de.

Received 21 January 2019

Returned for modification 1 March 2019

Accepted 10 June 2019

Accepted manuscript posted online 17 June 2019

Published 23 August 2019

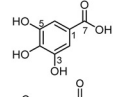
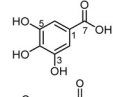
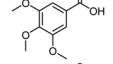
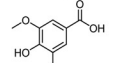
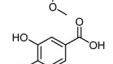
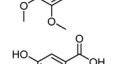
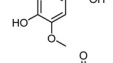
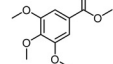
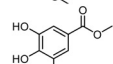
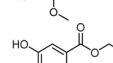
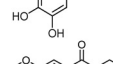
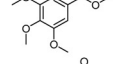
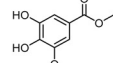
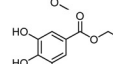
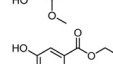
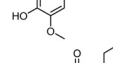
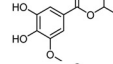
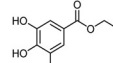
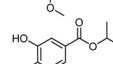
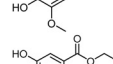
of 10 to 24 months, thereby tremendously increasing costs. In recent years, two new TB drugs, bedaquiline (BDQ) and delamanid, were conditionally approved for treatment of MDR TB infections but are still undergoing phase III clinical evaluations (3, 4). Nevertheless, new lead structures are still urgently needed since resistance against BDQ and delamanid has already been reported (5, 6). Since the discovery of penicillin (7), antibacterial compounds have been sought from natural sources such as plants and marine or soil-dwelling microorganisms, among many others. To date, approximately 70% of all available antibiotics have been derived from nature (8). The variety of secondary metabolites protecting plants from microbial enemies seems to be innumerable. The semiparasitic Nigerian mistletoe *Loranthus micranthus* is used in African traditional medicine for various indications (9–11). Among other activities, antibacterial effects of extracts from this plant have been reported also (12–15). Therefore, in this study, we investigated the antitubercular properties of compounds isolated from *L. micranthus* and characterized the anti-TB effect of identified natural alkylgallates and synthetic derivatives thereof.

(Parts of this study were included in a Ph.D. dissertation by N. Rehberg at Heinrich Heine University Düsseldorf.)

RESULTS

Isolation, antitubercular activity, and structure-activity relationships of gallic acid derivatives. In our screening efforts, an *n*-butanol extract of *L. micranthus* was prepared and subjected to various chromatographic separation steps, including final purification of natural products by semipreparative high-performance liquid chromatography (HPLC) to yield several known natural gallic acid derivatives (compounds 1 to 5, 8, and 10). These compounds were readily identified by comparison of their ¹H and ¹³C nuclear magnetic resonance (NMR) data to mass spectra reported in the literature and were identified as gallic acid (compound 1) (16), eudesmic acid (compound 2) (17), 3,5-di-*O*-methyl-gallic acid (compound 3) (18), 3,4-di-*O*-methyl-gallic acid (compound 4) (16), 3-*O*-methyl-gallic acid (compound 5) (14), butylgallate (compound 8) (19), and 3-*O*-methyl-butylgallate (compound 10) (20). Testing of these natural products for whole-cell activity against *M. tuberculosis* H37Rv revealed that 3-*O*-methyl-butylgallate (compound 10) exhibited strong antibacterial potency. Butylgallate (compound 8) showed much weaker activity, while all other tested derivatives were not active (Table 1). To reveal more insights into the structural determinants important for antibacterial activity, a variety of structural variants (compounds 6, 7, 9, and 11 to 19) were synthesized based on commercially available gallic acid derivatives as precursors. Of these synthetic compounds, 6, 7, 9, 12, 14, and 18 to 19 are known structures, which were identified by comparison of their ¹H and ¹³C NMR data to mass spectra in the literature and identified as 3,4,5-tri-*O*-methyl-methylgallate (compound 6) (17), 3-*O*-methyl-methylgallate (compound 7) (21), 3,4,5-tri-*O*-methyl-butylgallate (compound 9) (22), 3-*O*-methyl-octylgallate (compound 12) (23), 3-*O*-methyl-propylgallate (compound 14) (24), *N*-butyl-3,4-dihydroxy-5-methoxybenzamide (compound 18) (24), and *N*-hexyl-3,4-dihydroxy-5-methoxybenzamide (compound 19) (24). Compounds 11, 13, and 15 to 17 are new, and their structures have been confirmed by analysis of their ¹H NMR and MS data (see Fig. S1 to S10 in the supplemental material). All of the natural and synthetic compounds were tested for their antibacterial activity against *M. tuberculosis* H37Rv as well as against nosocomial pathogens, including *Staphylococcus aureus*, *Enterococcus faecalis*, *Enterococcus faecium*, and *Acinetobacter baumannii*. The antibacterial activity screening revealed that compounds 10, 11, and 12 were the most active against *M. tuberculosis* H37Rv, with a MIC of 6.25 μM (1.7 mg/liter). Structure-activity relationships (SAR) showed that compounds with a free carboxyl moiety (i.e., compounds 1 to 5) did not inhibit the growth of *M. tuberculosis* H37Rv or inhibited it only slightly (Table 1). Comparisons of data from compounds 7, 10 to 12, and 14 showed that esterification of the carboxyl group with medium-chain alcohols strongly enhanced their antitubercular activity. Increasing the level of lipophilicity by elongation of the aliphatic sidechain from propylgallate (compound 14) to butylgallate (compound 10)

TABLE 1 Structures of gallic acid derivatives, their antibacterial activity against *M. tuberculosis* H37Rv, and their cytotoxicity against the human cell lines THP-1 and MRC-5^a

	Compound		Concentration (μM)				
			<i>M. tb.</i> MIC ₉₀	THP-1 IC ₅₀ IC ₉₀		MRC-5 IC ₅₀ IC ₉₀	
1	Gallic acid		100	100	>100	100	>100
2	Eudesmic acid		>100	>100	>100	>100	>100
3	3,5-Di-O-methyl-gallic acid		>100	100	>100	>100	>100
4	3,4-Di-O-methyl-gallic acid		>100	>100	>100	>100	>100
5	3-O-Methyl-gallic acid		100	50	100	>100	>100
6	3,4,5-Tri-O-methyl-gallate		>100	>100	>100	>100	>100
7	3-O-Methyl-methylgallate		>100	100	>100	>100	>100
8	Butyl gallate		25	50	>100	>100	>100
9	3,4,5-Tri-O-methyl-butylgallate		>100	>100	>100	>100	>100
10	3-O-Methyl-butylgallate		6.25	100	100	>100	>100
11	3-O-Methyl-hexylgallate		6.25	50	100	>100	>100
12	3-O-Methyl-octylgallate		6.25	50	100	>100	>100
13	3-O-Methyl-cyclohexylgallate		>100	100	>100	>100	>100
14	3-O-Methyl-propylgallate		50	100	>100	>100	>100
15	3-O-Methyl-isopropylgallate		>100	>100	>100	>100	>100
16	3-O-Methyl-isobutylgallate		50	25	>100	100	>100
17	<i>N</i> -(2-Methyl-propyl)-3,4-dihydroxy-5-methoxybenzamide		100	100	>100	>100	>100
18	<i>N</i> -Butyl-3,4-dihydroxy-5-methoxybenzamide		>100	25	>100	100	>100
19	<i>N</i> -Hexyl-3,4-dihydroxy-5-methoxybenzamide		50	6.25	50	50	100

^aAntibacterial activity is shown as the concentration reducing bacterial growth by 90% relative to controls (MIC₉₀). Cytotoxicity is displayed as the concentrations reducing growth of human cells by 50% or 90% (IC₅₀ or IC₉₀ [indicated in micromoles], respectively) relative to controls.

resulted in augmented anti-TB potency, while further elongation to hexylgallate (compound 11) and octylgallate (compound 12) did not further increase potency. The results of analysis of butylgallate derivatives 8, 9 and 10 further demonstrated that methoxylation of the hydroxyl group at position 3 substantially increased antitubercular potency, while additional methoxylation of the hydroxyl groups at positions 4 and 5 was detrimental for antibacterial activity. Derivatives with sterically enlarged side chains such as 3-*O*-methyl-cyclohexylgallate (compound 13), 3-*O*-methyl-isopropylgallate (compound 15), and 3-*O*-methyl-isobutylgallate (compound 16) did not show any effect in the tested concentration range. Hence, a linear aliphatic chain seems to be essential for activity. Replacement of ester-linked alkyl chains with amine substituents (compounds 17 to 19) decreased the MIC, suggesting that the enlarged delocalized π -electron system in the amide derivatives reduced the level of interaction with the target. The common characteristics of the most active compounds comprise a methoxy group in *meta* position and an ester-linked linear aliphatic alkyl side chain consisting of four to eight carbon atoms.

Because previous studies had already reported on the antibacterial activity of some other alkylgallates against *B. subtilis*, *S. aureus*, and the Gram-negative bacterium *Xanthomonas citri* (25–28), we also checked the antibacterial effect of our compounds on several nosocomial strains. However, interestingly, only 3-*O*-methyl-octylgallate (compound 12) inhibited the growth of sensitive and resistant species of *Staphylococcus aureus* and *Enterococcus faecium*, although the inhibitory effect was weak, with MICs ranging from 25 to 100 μ M (see Table S1 in the supplemental material). Therefore, 3-*O*-methyl-alkylgallates display relatively specific antitubercular activity. In addition, *in vitro* cytotoxicity studies revealed that gallic acid derivatives were not cytotoxic toward the human cell lines THP-1 and MRC-5 or were only moderately cytotoxic, yielding a selectivity index (SI) (50% inhibitory concentration [IC₅₀]/MIC₉₀) value of ≥ 16 for compound 10 (Table 1). The most potent derivatives, compounds 10, 11, and 12, were additionally evaluated against a broader panel of human cell lines (HEPG2, CLS-54, HEK293, H4, HUH7), further corroborating their lack of cytotoxicity (Table S2).

***In vitro* killing kinetics.** Due to the fact that derivatives 10, 11, and 12 showed virtually equal levels of potency, we focused on 3-*O*-methyl-butylgallate (derivative 10) for all further characterizations of the antitubercular effect since it possessed the highest solubility of the three compounds. First, an assay of killing kinetics was performed. 3-*O*-Methyl-butylgallate, in monotherapy, showed a moderate bactericidal effect, with an $\sim 99\%$ reduction of viability after 10 days (Fig. 1A). After that time point, however, bacterial growth resumed. Individual clones isolated after 3 weeks of incubation were still fully sensitive toward the compound. This specifically contrasts with the tested first-line drug INH, which exhibited strong bactericidal killing effects after 4 days but was associated with outgrowth of resistant mutants after 3 weeks (Fig. 1E). This indicated that regrowth in the 3-*O*-methyl-butylgallate-treated culture was caused by compound depletion or degradation and not by development of resistances. Because TB chemotherapy relies on a combination treatment that includes the use of several drugs, the effects of combining 3-*O*-methyl-butylgallate (10) with the first-line drugs EMB, RIF, and INH or the new conditionally approved second-line agents BDQ and delamanid were investigated (Fig. 1B to F). In combination with EMB or BDQ, compound 10 caused an additive effect and delayed or prevented the outgrowth of mutants that was observable in monotherapy with EMB or BDQ, respectively (Fig. 1B and D). Combination of RIF or INH or delamanid with 3-*O*-methyl-butylgallate caused a synergistic killing effect (Fig. 1C, E, and F, respectively). In case of delamanid, the combination first reduced the number of bacteria to the detection limit of 10¹ CFU/ml. However, after 3 weeks, bacterial regrowth was observable (Fig. 1F). Interestingly, these clones exhibited resistance only against delamanid and not against 3-*O*-methyl-butylgallate, indicating that repeated addition of compound 10 to the culture might be able to prolong and increase this synergistic killing effect.

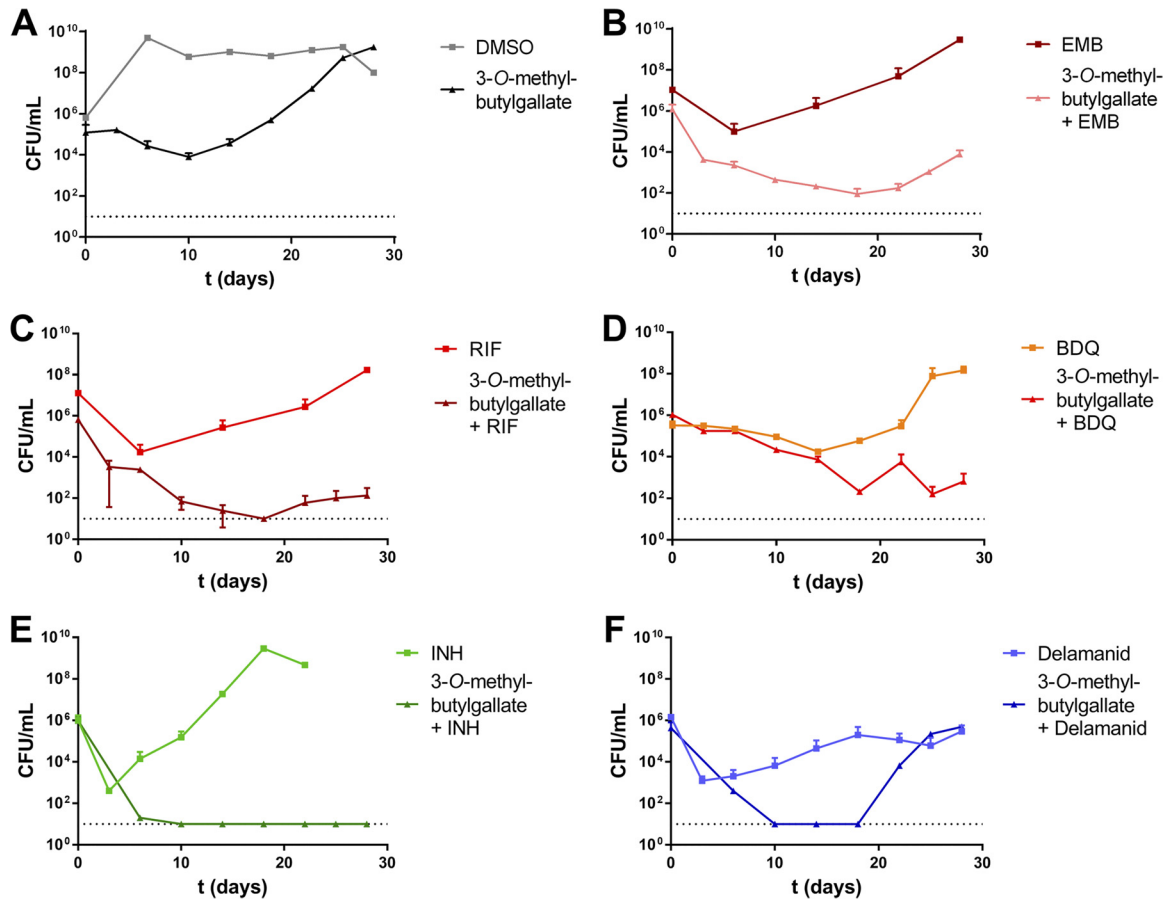


FIG 1 Time-killing curves of *M. tuberculosis* H37Rv in 3-O-methyl-butylgallate–drug combination treatments. (A) 3-O-Methyl-butylgallate (31.25 μ M) (square) and solvent control 3.1% DMSO (triangle). (B) Ethambutol (EMB) (10 μ M) (square) and combination of 10 μ M EMB and 31.25 μ M 3-O-methyl-butylgallate (triangle). (C) Rifampin (RIF) (1 μ M) (square) and combination of 1 μ M RIF and 31.25 μ M 3-O-methyl-butylgallate (triangle). (D) Bedaquiline (BDQ) (0.5 μ M) (square) and combination of 0.5 μ M BDQ and 31.25 μ M 3-O-methyl-butylgallate (triangle). (E) Isoniazid (INH) (10 μ M) (square) and combination of 10 μ M INH and 31.25 μ M 3-O-methyl-butylgallate (triangle). (F) Delamanid (0.5 μ M) (square) and combination of 0.5 μ M delamanid and 31.25 μ M 3-O-methyl-butylgallate (triangle). The limit of detection (indicated by the dotted line) was 10 CFU/ml in all experiments. Data represent means of duplicate measurements. Experiments were repeated once with similar results.

INH combined with 3-O-methyl-butylgallate revealed a strong synergistic killing effect leading to complete sterilization of the culture after 1 week (Fig. 1E). This interaction was also investigated in a checkerboard assay by determination of the fractional inhibitory concentration indices (FICI) for combination of 3-O-methyl-butylgallate with RIF or delamanid or INH. The presence of RIF at 0.25 \times MIC (0.078 μ M) revealed a partial synergistic effect (FICI = 0.562), resulting in increased sensitivity to 3-O-methyl-butylgallate (16-fold reduction in MIC). In contrast, combination with delamanid (0.146 μ M) or INH (0.156 μ M), with each at 0.25 \times MIC, resulted in synergism (FICI < 0.5) and strongly increased sensitivity to 3-O-methyl-butylgallate (Table S3).

Several *M. tuberculosis* clinical isolates (CDC1551, Erdman, and HN878) as well as XDR strains originating from South Africa were tested for susceptibility to 3-O-methyl-butylgallate. While *M. tuberculosis* strain Erdman showed sensitivity equal to that seen with H37Rv, strain CDC1551 was even more susceptible. In contrast, Beijing strain HN878 exhibited 8-fold-lower sensitivity, whereas all tested XDR strain isolates exhibited high-level resistance (see Fig. S11), indicating that this compound might have limited clinical application only for treatment of infections with drug-sensitive strains.

Mode of action and resistance mechanism. To get insights into the mode of action, the molecular target(s), and the possible mechanisms of resistance of 3-O-methyl-alkylgallates, spontaneous resistant mutants of *M. tuberculosis* H37Rv were

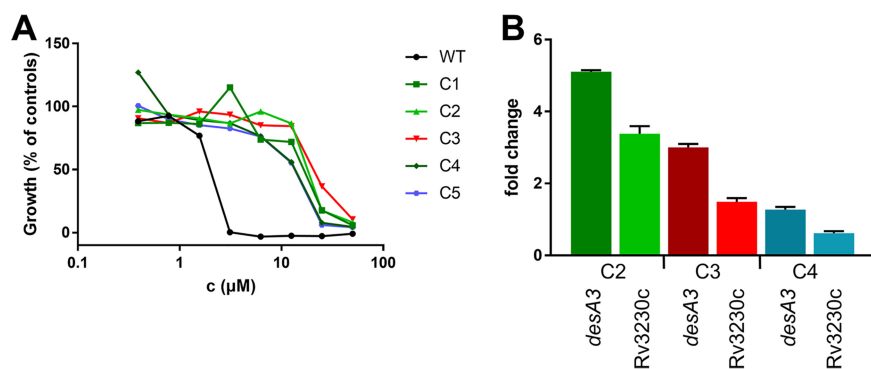


FIG 2 Characterization of spontaneously 3-*O*-methyl-butylgallate-resistant mutants of *M. tuberculosis* H37Rv (C1 to C5). (A) Dose-response curves of 3-*O*-methyl-butylgallate-resistant mutants in comparison to the sensitive WT strain. Growth levels were quantified using the resazurin dye reduction assay and calculated relative to controls. Data represent single measurements. (B) Expression of *desA3* and *Rv3230c* in spontaneously resistant clones C2, C3, and C4 in comparison to the WT strain. The transcription level was quantified using GoTaq qPCR Master Mix and a CFX96 real-time system and calculated relative to the WT control and normalized to 16S rRNA. For all calculations, the Livak method was used.

isolated on solid medium containing 3-*O*-methyl-butylgallate at 5× MIC, which occurred at a frequency of 3.3×10^{-7} . Five independent mutants were randomly selected for further characterization. All clones exhibited an 8-fold to 16-fold shift in MIC for 3-*O*-methyl-butylgallate and were also cross-resistant to 3-*O*-methyl-hexylgallate and 3-*O*-methyl-octylgallate (Fig. 2A; see also Fig. S12). Subsequently, the resistance-mediating mutations were mapped by employing whole-genome sequencing. Three of the mutants (C1, C2, and C5) harbored duplications of a common region spanning genes *Rv3208* to *Rv3324*. Two clones (C3 and C4) exhibited a single nucleotide polymorphism (SNP) in the putative promoter region of gene *Rv3230c*, which is part of the duplicated regions found in the aforementioned mutants (Table 2). Three of these mutants harbored additional SNPs in other loci such as genes involved in phthiocerol dimycocerosate (PDIM) biosynthesis (*ppsC* or *mas*). Mutations in PDIM biosynthesis are known to occur frequently during *in vitro* culture (29) and were thus estimated to be unrelated to resistance (Table 2).

In light of these findings, the possible resistance mechanism in the studied mutants might be overexpression of gene *Rv3230c* and/or downstream gene *Rv3229c*, which forms a two-gene operon with *Rv3230c*. This overexpression might have occurred either by gene duplication or as a consequence of the presence of a SNP in the promoter region upstream of *Rv3230c*. In fact, quantitative PCR (qPCR) analyses of resistant mutants C2, C3, and C4 confirmed that genes *Rv3229c* and *Rv3230c* were both overexpressed compared to the wild-type (WT) strain results (Fig. 2B). *Rv3229c* (*desA3*) encodes one of the three aerobic desaturases (DesA1, DesA2, and DesA3) present in the genome of *M. tuberculosis* H37Rv (30). The integral membrane stearyl-coenzyme A (stearyl-CoA) desaturase DesA3 and the corresponding oxidoreductase *Rv3230c* con-

TABLE 2 Mutations in 3-*O*-methyl-butylgallate-resistant *M. tuberculosis* H37Rv mutants identified by whole-genome sequencing

3- <i>O</i> -Methyl-butylgallate-resistant mutant	Gene mutation(s): SNP or length of duplication ^a
C1	306-kb duplication (<i>Rv3208</i> – <i>Rv3473c</i>)
C2	146-kb duplication (<i>Rv3188</i> – <i>Rv3324</i>); G → A 154-bp upstream of <i>mas</i>
C3	T → G 61 bp upstream of <i>Rv2576c</i> ; for <i>ppsC</i> , +C in aa 897; G → T 23 bp upstream of <i>Rv3230c</i>
C4	T → G 61 bp upstream of <i>Rv2576c</i> ; for <i>ppsC</i> , +C in aa 897; G → T 23 bp upstream of <i>Rv3230c</i> ; C → T 10 bp upstream of <i>Rv2652c</i>
C5	146-kb duplication (<i>Rv3188</i> – <i>Rv3324</i>)

^aNucleotides listed are based on the positive strand.

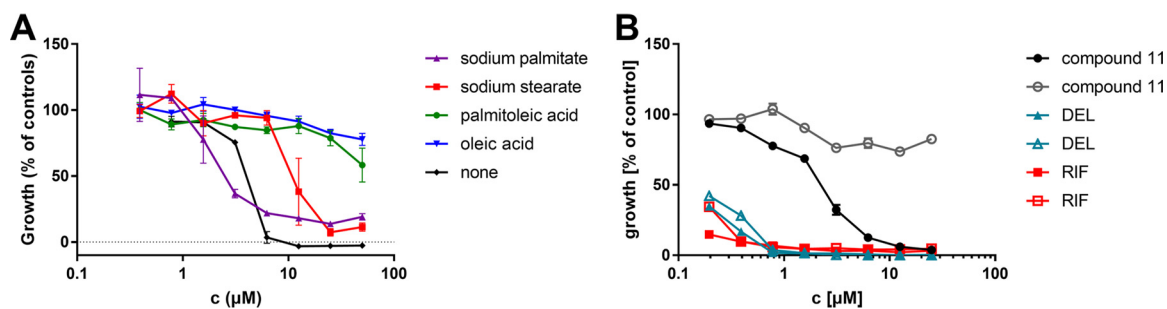


FIG 3 Effect of fatty acid supplementation on drug sensitivity of *M. tuberculosis* H37Rv. (A) Dose-response curves of 3-O-methylbutylgallate during supplementation with sodium palmitate (triangle), sodium stearate (square), palmitoleic acid (circle), or oleic acid (reversed triangle) (each at a final concentration of 0.05 g/liter) or without supplementation (rhombus). Growth levels were quantified using the resazurin dye reduction assay. Data represent means of results from experiments performed in triplicate \pm standard deviations (SD). (B) Control experiment with antitubercular drugs delamanid (DEL; triangle) and rifampin (RIF; rhombus) as well as compound 11 (circle). Medium was supplemented with oleic acid (open symbols) or left without supplementation (filled symbols).

vert saturated stearic acid to unsaturated oleic acid using molecular oxygen and NADPH for synthesis (30, 31).

To investigate a possible role of altered fatty acid desaturation in resistance, the influence of various fatty acids on the sensitivity of *M. tuberculosis* to 3-O-methylalkylgallates during supplementation to the medium was tested. The supplementation with the unsaturated fatty acids palmitoleic acid and oleic acid completely abolished the inhibitory activity of the tested 3-O-methylalkylgallates in the tested concentration range. In contrast, supplementation with the corresponding saturated derivatives palmitate and stearate did not decrease the sensitivity of the cells or decreased it only slightly. In control experiments, oleic acid did not affect the sensitivity of *M. tuberculosis* H37Rv to RIF or delamanid. These findings support the conclusion that 3-O-methylalkylgallates specifically inhibit the fatty acid desaturation pathway without causing relevant off-target effects (Fig. 3; see also Fig. S13A and B).

A previous study suggested that the antibiotic isoxyl (ISO), which had been clinically used in the treatment of TB in the past, also inhibits DesA3 activity (32). Supporting this assumption, similarly to our observations, addition of oleic acid to the medium partially restored growth of ISO-treated *M. tuberculosis* cells on solid medium (32). However, a direct physically interaction of ISO with purified DesA3 has not been demonstrated. In contrast, a more recent study suggested that inhibition of the (3R)-hydroxyacyl-acyl carrier protein dehydratases encoded by *hadABC*, thereby targeting FAS-II-mediated mycolic acid rather than fatty acid desaturation, is more relevant than DesA3 inhibition for the antitubercular activity of ISO (33). Supporting the latter hypothesis, our own investigations confirmed that supplementation with fatty acids did not antagonize the inhibitory effect of ISO against *M. tuberculosis* H37Rv in liquid culture *in vitro* (Fig. S13C). Additionally, the lack of cross-resistance of spontaneous 3-O-methylbutylgallate-resistant mutants to ISO indicates that similarities between the putative targets of gallic acid derivatives and ISO are unlikely (data not shown).

In vitro drug-like properties of 3-O-methylbutylgallate. In order to perform a first assessment of drug-like properties of 3-O-methylbutylgallate, levels of interaction with P-glycoprotein (P-gp) and CYP enzymes was estimated, logP values were calculated, and permeability (P_{app}) was determined in the Caco2 model. 3-O-Methylbutylgallate did not inhibit P-gp in the calcein assay, whereas verapamil as a positive control, with an IC_{50} of 13.3 μ M, showed inhibition (Fig. 4A). Furthermore, 100 μ M 3-O-methylbutylgallate inhibited CYP3A4 by 47% (Fig. 4B) but did not significantly inhibit CYP1A2 and CYP2B6 (not shown). The logP value was calculated as 2.84 according to a method described previously by Daina et al. (34). Finally, the permeability of 3-O-methylbutylgallate was estimated in the Caco2 monolayer system. 3-O-Methylbutylgallate gave a P_{app} value of 6.2×10^{-6} cm/s, suggesting mediocre absorption. As a positive control, the P_{app} value for diclofenac, a well-absorbed drug, was estimated as 43×10^{-6} cm/s. Based on these

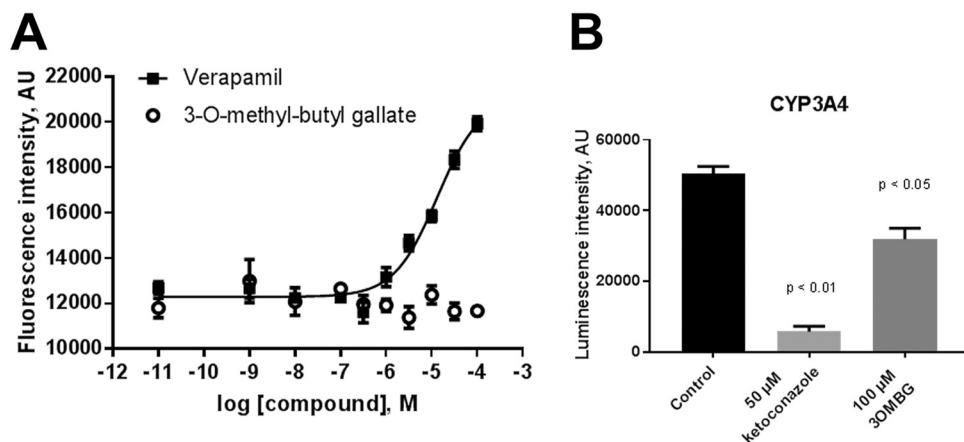


FIG 4 *In vitro* drug-like properties of 3-*O*-methyl-butyl-gallate. (A) Effect of 3-*O*-methyl-butylgallate on P-gp-mediated efflux of calcein-AM compared to verapamil. Increasing concentrations of 3-*O*-methyl-butylgallate were incubated with P-gp-expressing CaCo2 cells followed by analysis of intracellular calcein fluorescence. Verapamil was used as a positive control. 3-*O*-Methyl-butylgallate did not show any interaction with calcein fluorescence, indicating that there was no interaction with P-gp. Data shown represent means \pm standard errors of the means (SEM); $n = 3$. (B) Effect of 3-*O*-methyl-butylgallate (3OMBG) on inhibition of CYP3A4. CYP3A4 specific substrates have been used and ketoconazole was used as selective control inhibitor. Data shown represent means \pm SEM of results from 3 experiments. AU, arbitrary units.

collective preliminary results, 3-*O*-methyl-butylgallate has favorable absorption, distribution, metabolism, and excretion (ADME) parameters, qualifying this compound for further evaluation as an antitubercular compound.

DISCUSSION

The results of this study strongly indicate that the plant natural product 3-*O*-methyl-butylgallate specifically inhibits growth of *M. tuberculosis* H37Rv by targeting the stearoyl desaturase DesA3. DesA3 is one of the three aerobic desaturases present in the genome of *M. tuberculosis* H37Rv (30). The two homologs DesA1 and DesA2 are predicted to have a specific role in mycolic acid biosynthesis, as they encode putative acyl-ACP desaturases that might introduce double bonds into the mero chain of mycolic acids after those have been formed by the FAS-II enzyme complex (35, 36). In contrast, the integral membrane stearoyl-CoA desaturase DesA3, forming a functional complex with the corresponding oxidoreductase Rv3230c, converts saturated stearic acid to unsaturated oleic acid by the use of molecular oxygen and NADPH for synthesis (30, 31). Oleic acid plays a crucial role in membrane composition for maintenance of physiological functions. Incorporation of unsaturated fatty acid into membrane lipids regulates membrane fluidity (32). In addition, mycolic acid synthesis is believed to require oleic acid as a precursor for introduction of double bonds into certain mycolic acid structures (37). This implies that DesA3 and Rv3230c might be essentially involved in lipid metabolism for both cell membrane and cell wall formation in *M. tuberculosis*. Due to the strong compensation of the inhibitory effect of 3-*O*-methyl-alkylgallates by oleic acid supplementation, specific targeting of DesA3 and/or Rv3230c seems very likely, although more studies are required to confirm and characterize the postulated compound-target interaction. Paradoxically, *desA3* has been described previously in *M. tuberculosis* H37Rv as a nonessential gene in genome-wide saturated transposon mutant screens (38). However, the medium used for selection of mutants in that study was supplemented with OADC (oleic acid-albumin-dextrose-catalase) enrichment, yielding a final oleic acid concentration of 0.05 g/liter, which was sufficient to chemically complement the genetic defect. No reports are available on the viability of defined *desA3* deletion mutants in animal infection models. However, genome-wide saturated transposon mutant screens revealed that *desA3* is essential for growth of *M. tuberculosis* H37Rv in C57BL/6J mouse spleen (39). This indicates that *M. tuberculosis* cannot acquire

sufficient amounts of oleic acid or other suitable unsaturated fatty acids from the host, thus corroborating identification of DesA3 as a vulnerable target during infection.

In general, stearoyl desaturases have been described as the molecular targets of structurally unrelated compounds that inhibit growth of *Toxoplasma gondii* or cancer progression, for instance (40, 41). None of these compounds have been reported to exhibit antitubercular activity. The synthetic compound isoxyl, which had been clinically used in the treatment of TB in the past, was initially believed to inhibit DesA3 activity (32). A more recent study, however, indicated that inhibition of the (3*R*)-hydroxyacyl-acyl carrier protein dehydratases encoded by *hadABC* is more relevant for the antitubercular activity of isoxyl, thereby targeting FAS-II-mediated mycolic acid rather than fatty acid desaturation (33). Therefore, 3-O-methyl-butylgallate might represent the first specific inhibitor of *M. tuberculosis* DesA3.

Nonmethylated alkylgallates were described previously in the literature as antibacterial compounds which inhibit growth of *Bacillus subtilis*, *S. aureus*, and the Gram-negative plant pathogen *Xanthomonas citri* (25, 27, 28). Also, the inhibitory effect of ethyl gallate on *M. tuberculosis* had already been described previously (42). However, the reported activities of these nonmethylated derivatives were rather low. In fact, a study investigating 3-O-acetylated alkylgallates was published recently, demonstrating that acetylation increases potency against *Xanthomonas citri* (43). The published data indicate that filamentation temperature-sensitive protein Z (FtsZ) and permeabilization of bacterial membranes represent potential drug targets of alkylgallates in these bacteria. FtsZ is a self-activating GTPase that polymerizes at the future site of divisions, forming a ring, and is essential for cell division in bacteria. It was postulated that the effect of alkylgallates on FtsZ in *X. citri* might be indirect and might be mediated by disturbing membrane integrity due to the surfactant properties of the gallic acid derivatives, thereby dislocating FtsZ from the membrane (26, 44). In addition to membrane permeabilization, a direct interaction of alkylgallates with FtsZ was demonstrated for *B. subtilis* also (28). However, 3-O-methyl-alkylgallates have a rather specific effect on *M. tuberculosis* and not on other bacteria. Also, targeting of FtsZ in *M. tuberculosis* would not easily explain the compensatory effect of oleic acid on the antitubercular activity of 3-O-methyl-alkylgallates. Therefore, the possible involvement of FtsZ in the processes that explain the antibacterial effect of 3-O-methyl-alkylgallates on *M. tuberculosis* has to be assessed in further studies.

Several tested *M. tuberculosis* XDR strains as well as a strain from the Beijing lineage were resistant to 3-O-methyl-butylgallate, indicating that this compound might have limited clinical application for treatment of infections with drug-sensitive strains only. Nevertheless, the observed pronounced synergistic killing effects with RIF and INH suggest a promising alternative to TB standard therapy which might shorten treatment durations for infections by drug-susceptible *M. tuberculosis* strains. Further studies are required to evaluate the *in vivo* efficacy of 3-O-methyl-alkylgallates and their clinical applicability and usefulness.

MATERIALS AND METHODS

Isolation and structure elucidation of gallic acid derivatives from *Loranthus micranthus*. The leaves of Nigerian mistletoe (*Loranthus micranthus*), which is parasitic on the host tree *Kola acuminata*, were collected from Orba Nsukka in Enugu State, Nigeria, in February 2015 and authenticated by a plant taxonomist, Alfred Ozioko of the Bio-resource Development and Conservation Program (BDPC), Nsukka, Nigeria. A voucher specimen of the sample is stored at the center with number BDC-1021-015B. The leaves were dried in the shade for 8 days and then pulverized to a fine powder using a laboratory grinder. A total of 3.0 kg of the powdered plant material was macerated repeatedly with distilled water (total volume, 12 liters). The resulting aqueous extract was lyophilized under vacuum, affording a dry powdered extract with a total yield of 723 g. The dry extract was then partitioned between water and *n*-hexane followed by partitioning between water and EtOAc and finally between water and *n*-butanol. The *n*-butanol fraction (total yield, 150 g), which turned out to be the most active fraction in the bioassays with *M. tuberculosis*, was then subjected to separation by vacuum liquid chromatography (VLC) on a silica gel (200 to 400 mesh) using a gradient of hexane/EtOAc (100:0 [1.5 liters], 90:10 [1.0 liters], 80:20 [1.0 liters], 60:40 [1.0 liters], 40:60 [1.0 liters], 20:80 [500 ml], and 0:100 [500 ml]) to afford VLC fractions BU01 to BU07 and a gradient of CH₂Cl₂/MeOH (100:0 [500 ml], 80:20 [1.0 liters], 60:40 [1.0 liters], 40:60 [1.0 liters], 20:80 [1.0 liters], and 0:100 [1.0 liters]) to afford VLC fractions BU08 to BU13. All VLC

fractions were screened for antimicrobial and cytotoxicity activities, and fraction BU05 (71.9 mg) showed the highest activity. That fraction was subsequently subjected to semipreparative HPLC using a Merck Hitachi L-7100 pump (Merck/Hitachi, Germany) coupled to a UV detector (L-7400). A linear gradient of HPLC-grade methanol and nanopure water was used for separation, affording gallic acid (compound 1), eudesmic acid (compound 2), 3,5-di-*O*-methyl-gallic acid (compound 3), 3,4-di-*O*-methyl-gallic acid (compound 4), 3-*O*-methyl-gallic acid (compound 5), butylgallate (compound 8), and 3-*O*-methyl-butylgallate (compound 10) as pure constituents. The structural identity of the compounds was confirmed by one-dimensional and two-dimensional NMR and by mass spectroscopy.

Synthesis of gallic acid esters 6, 7, 9, and 11 to 16. For the preparation of compounds 7 and 11 to 16, eight aliquots of 3-*O*-methyl-gallic acid (Sigma-Aldrich, Germany) (36.8 mg, 0.2 mmol) were dissolved in 5 ml of respective alcohol reaction mixtures, followed by dropwise addition of three equivalents of SOCl_2 (40 μl , 0.6 mmol). The resulting solution was heated under reflux conditions for 8 h and then concentrated *in vacuo*. EtOAc was added, and the solution was dried over anhydrous MgSO_4 . After removing the solvent, the respective 3-*O*-methyl-gallic acid ester was obtained. To prepare compounds 6 and 9, 3,4,5-tri-*O*-methyl-gallic acid (Sigma-Aldrich, Germany) was used instead of 3-*O*-methyl-gallic acid (45).

Synthesis of gallic acid amides 17 to 19. 3-*O*-Methyl-gallic acid (36.8 mg, 0.2 mmol) was dissolved in 5 ml of SOCl_2 at room temperature and stirred for 5 min. Then the reaction solution was heated under reflux conditions for 2 h. The solvent was removed, and the residue was dissolved in 0.1 ml of tetrahydrofuran (THF). The resulting solution was then added to 1 ml of respective amine and stirred for 20 min at room temperature. The solvent was removed under reduced pressure to give amides 17 to 19 (45).

Bacterial strains and growth conditions. Cells of *M. tuberculosis* strains H37Rv, CDC1551, Erdman, and HN878 and of several XDR-TB clinical isolates from South Africa (29) were grown aerobically in Middlebrook 7H9 medium containing 10% (vol/vol) ADS enrichment solution (5% [wt/vol] bovine serum albumin [fraction V], 2% [wt/vol] glucose, 0.85% [wt/vol] sodium chloride), 0.5% (vol/vol) glycerol, and 0.05% (vol/vol) tyloxapol at 37°C. XDR-TB clinical strains originating from South Africa were obtained from William R. Jacobs, Jr, (Albert Einstein College of Medicine, Bronx, USA), and exhibited the following resistance levels: 1 mg/liter isoniazid, 1 mg/liter rifampin, 10 mg/liter ethambutol, 2 mg/liter streptomycin, 100 mg/liter pyrazinamide, 5 mg/liter ethionamid, 5 mg/liter kanamycin, 4 mg/liter amikacin, 10 mg/liter capreomycin, and 2 mg/liter ofloxacin.

Nosocomial bacterial strains were cultivated in Mueller-Hinton (MH) medium at 37°C and included methicillin-susceptible *S. aureus* (MSSA) strain ATCC 25923 and methicillin-resistant *S. aureus*/vancomycin-intermediate *S. aureus* (MRSA/VISA) strain ATCC 700699; *E. faecalis* strains ATCC 29212 and ATCC 51299 (vancomycin resistant); *Enterococcus faecium* strains ATCC 35667 and ATCC 700221 (vancomycin resistant); and *Acinetobacter baumannii* strain ATCC BAA 1605 (MDR).

Determination of MIC against *M. tuberculosis* via resazurin dye reduction method. For the determination of drug MICs against *M. tuberculosis*, bacteria were precultured until the log phase (optical density at 600 nm [OD_{600}] = 0.5 to 1) and were then seeded at 1×10^5 cells per well in a total volume of 100 μl in 96-well round-bottom microtiter plates and incubated with 2-fold serially diluted compounds at a concentration range of 100 to 0.78 μM . Microplates were incubated at 37°C for 5 days essentially as described previously (46). Afterward, 10 μl /well of a 100 $\mu\text{g}/\text{ml}$ resazurin solution was added and incubated at ambient temperature for further 16 h. Then cells were fixed for 30 min after formalin addition (5% [vol/vol] final concentration). For viability determinations, fluorescence was quantified using a microplate reader (excitation, 540 nm; emission, 590 nm). Percentages of growth were calculated relative to rifampin-treated (0% growth) and dimethyl sulfoxide (DMSO)-treated (100% growth) controls.

For chemical complementation experiments, the medium was individually supplemented with a fatty acid (sodium palmitate or sodium stearate or palmitoleic acid or oleic acid, each at a final concentration of 0.05 g/liter), while all other parameters of the assay remained the same.

Determination of MIC against nosocomial strains. MICs of gallates for various typical nosocomial bacterial pathogens (*Staphylococcus aureus*, *Enterococcus faecalis*, *Enterococcus faecium*, *Acinetobacter baumannii*) were determined by the broth microdilution method according to the recommendations of the Clinical and Laboratory Standards Institute (CLSI) (47). For preparation of the inoculum, the growth method was used. Bacterial cells were grown aerobically in MH medium at 37°C and 180 rpm. A preculture was grown until the log phase was reached (OD_{600} of ~ 0.5) and then seeded at 5×10^4 bacteria/well in a total volume of 100 μl in 96-well round-bottom microtiter plates and incubated with 2-fold serially diluted compound at a concentration range of 100 to 0.78 μM . Microplates were incubated aerobically at 37°C for 24 h. MICs were determined macroscopically by identifying the minimum concentration of the compound that led to complete inhibition of visual growth of the bacteria.

Determination of cytotoxicity and therapeutic index. The cytotoxicity of the compounds was determined *in vitro* using human monocyte cell line THP-1 (Deutsche Sammlung von Mikroorganismen und Zellkulturen GmbH), human fetal lung fibroblast cell line MRC-5 (American Type Culture Collection), human hepatoblastoma cell lines HepG2 and HuH7, human brain neuroglioma cell line H4, human lung carcinoma epithelial cell line CLS-54, and human embryonic kidney epithelial cell line HEK293 (all from CLS Cell Lines Service GmbH, Eppelheim, Germany). THP-1, CLS-54, and HuH7 cells were cultured in RPMI 1640 medium containing 10% (vol/vol) heat-inactivated fetal bovine serum (FBS). H4 cells were incubated in Dulbecco's modified Eagle's medium (DMEM) containing 10% (vol/vol) FBS. HepG2 cells were cultivated in Ham's F12 medium supplemented with 2 mM L-glutamine and 10% (vol/vol) FBS. MRC-5 cells were cultivated in Eagle's minimum essential medium (EMEM) supplemented with 1 mM sodium pyruvate and 10% (vol/vol) FBS. HEK293 cells were cultivated in EMEM supplemented with 2 mM L-glutamine, 1% (vol/vol) nonessential amino acids, 1 mM sodium pyruvate, and 10% (vol/vol) FBS. All cell

lines were incubated at 37°C in a humidified atmosphere of 5% CO₂. Cells were seeded at approximately 5×10^4 cells/well in a total volume of 100 μ l in 96-well flat-bottom microtiter plates containing 2-fold serially diluted compound at a maximum final concentration of 100 μ M. Cells treated with DMSO at a final concentration of 1% (vol/vol) served as solvent controls. After an incubation time of 48 h, 10 μ l resazurin solution (100 μ g/ml) was added per well, and the contents of the wells were incubated for a further 3 h at 37°C in a humidified atmosphere of 5% CO₂. Fluorescence was quantified using a microplate reader (excitation, 540 nm; emission, 590 nm). Growth was calculated relative to noninoculated (i.e., cell-free) (0% growth) and untreated (100% growth) controls in triplicate experiments, respectively. For determination of the therapeutic index of the substance, the selectivity index (SI) was determined by the quotient of cytotoxic concentration and MIC.

Determination of time-kill curves *in vitro*. Bacterial cells were grown aerobically at 37°C in 10 ml Middlebrook 7H9 liquid media supplemented with 0.5% (vol/vol) glycerol, 0.05% (vol/vol) tyloxapol, and 10% (vol/vol) ADS enrichment as shaking cultures. Exponentially growing cultures were diluted to a titer of ca. 1×10^6 CFU/ml as estimated from optical density measurements performed on the basis of the calculation that an OD₆₀₀ of 1 translates to 3×10^8 CFU/ml. Compound 10 was added at a concentration of 31.25 μ M ($5 \times \text{MIC}_{100}$) either alone or in combinations with individual clinical drugs (1 μ M rifampin, 10 μ M isoniazid, 10 μ M ethambutol, 0.5 μ M bedaquiline, and 0.5 μ M delamanid). Culture aliquots were taken at different time points, and 10-fold serial dilutions were plated on Middlebrook 7H10 agar plates to count viable cells after 3 weeks of incubation at 37°C. To check the outgrowth of spontaneous resistant mutants after 3 weeks, aliquots were plated out on compound-containing agar.

Checkerboard synergy assay. The fractional inhibitory concentration index (FICI) values for compound 10 with isoniazid, delamanid, or rifampin were determined in a 96-well plate format employing 2-dimensional dilutions of compounds. *M. tuberculosis* strain H37Rv was seeded at 10^5 CFU/well in a total volume of 100 μ l and incubated at 37°C for 5 days. For quantification, the resazurin assay was used as described above. The FICI value was calculated as the sum of the quotients of the lowest inhibitory concentration in a row (A and B, respectively) and the MIC of the compound (MIC_A and MIC_B, respectively) as follows:

$$\text{FICI} = \frac{\text{A}}{\text{MIC}_A} + \frac{\text{B}}{\text{MIC}_B}$$

Total synergism (FICI \leq 0.5), partial synergism (0.5 < FICI \leq 0.75), no effect (0.75 < FICI \leq 2), or antagonism (FICI > 2) between chlorflavonin and the tested antibiotics was deduced from the observed FICI values (48).

Determination of single-step resistance frequency. Spontaneous resistant mutants were isolated by plating approximately 1×10^8 CFU on agar (1 ml per well in a 6-well microtiter plate) containing compound 10 at $5 \times \text{MIC}$. Spontaneous resistant colonies were obtained at a frequency of ca. 1×10^{-7} after 3 weeks of incubation at 37°C. Five independent clones were selected, and all five exhibited moderate resistance against compounds 10, 11, and 12 in liquid culture.

Whole-genome sequencing. To identify the resistance-mediating mutations, genomic DNA was isolated from five independent mutants as described previously (49). Libraries were prepared for sequencing using a standard paired-end genomic DNA sample preparation kit from Illumina. Genomes were sequenced using an Illumina HiSeq 2500 next-generation sequencer (San Diego, CA, USA) and compared with the parent *M. tuberculosis* H37RvMA genome (GenBank accession no. GCA_000751615.1). Paired-end sequence data were collected with a read length of 106 bp. Base-calling was performed using Casava software, v1.8. The reads were assembled using a comparative genome assembly method and *M. tuberculosis* H37RvMA as a reference sequence (29). The mean depth of coverage ranged from 277 \times to 770 \times .

qPCR analysis. For reverse transcription-quantitative PCR (qRT-PCR), DNA-free total RNA samples were prepared from wild-type cells and spontaneously resistant clones C2, C3, and C4. An RNeasy minikit (Qiagen, Hilden, Germany) was used for RNA preparation, and a SuperScript III first-strand synthesis system (Invitrogen, Carlsbad, CA, USA) was used for reverse transcription of RNA to cDNA. From each primer, 250 nM and 10 μ l of template reaction (1:10 dilution) were utilized in 50- μ l reaction mixtures with GoTaq qPCR Master Mix (Promega, Mannheim, Germany). Triplicate samples were run on a CFX96 real-time system (Bio-Rad, Düsseldorf, Germany). Thresholds were normalized to 16S rRNA.

Calcein-AM assay for determination of pgp activity. Caco-2 cells (Deutsche Sammlung von Mikroorganismen und Zellkulturen GmbH) were grown in MEM supplemented with 20% fetal bovine serum at 37°C in a humidified atmosphere of 5% CO₂. Approximately 20,000 cells were seeded into wells of a 96-well plate and grown overnight. Compounds were then added in 3.6-fold dilutions from 1 nM to 100 μ M and incubated for 30 min. Then, 0.3 μ M calcein acetoxyethyl (calcein-AM) was added to each well, and fluorescence (excitation, 485 nm; emission, 520 nm) was monitored for 40 min. Fluorescence at 40 min was used as a readout to construct concentration-effect curves. Verapamil served as a positive-control inhibitor of Pgp.

Permeability assay in Caco-2 cells. Caco-2 cells were used to estimate P_{app} values for test compounds according to a detailed protocol described previously by Hubatsch et al. (50). Briefly, approximately 300,000 cells were seeded per well of a Corning Costar insertion transwell. After 22 to 24 days, a monolayer has been formed, and the apical to basolateral permeability experiment was performed. Compounds (diclofenac or 3-O-methyl-butylgallate) (5 μ M) were added to the apical compartment of the transwell chamber. After 30, 60, and 90 min, samples of the basolateral compartment were drawn and analyzed by HPLC. The P_{app} values were calculated as P_{app} = (dQ/dt) \times [1/(A \times C₀)],

where dQ/dt represents the steady-state flux in micromoles per second, A is the surface area of the filter, and C_0 is the initial concentration of the apical donor chamber.

Cytochrome P450 inhibition assays. CYP1A2, CYP2B6, and CYP3A4 inhibition assay kits were bought from Promega (Mannheim, Germany). The respective CYP enzymes were incubated with 20, 50, and 100 μ M test compounds. Then, subtype-specific derivatives of beetle luciferin were added according to the protocol of the manufacturer and luminescence was estimated using a BMG Lumistar reader. Positive controls were as follows: ciprofloxacin for CYP1A2, clopidogrel for CYP2B6, and ketoconazole for CYP3A4.

SUPPLEMENTAL MATERIAL

Supplemental material for this article may be found at <https://doi.org/10.1128/AAC.00136-19>.

SUPPLEMENTAL FILE 1, PDF file, 1.6 MB.

ACKNOWLEDGMENTS

This work was supported by the Deutsche Forschungsgemeinschaft (DFG; German Research Foundation [project number 270650915/GRK 2158] [to R.K. and P.P.]), by the Manchot Foundation (P.P.), and by the Federal Ministry of Education and Research BMBF (grant 16GW0109 [R.K.] and grant 16GW0108 [M.U.K.]).

REFERENCES

- WHO. 2017. Global tuberculosis report. WHO, Geneva, Switzerland.
- Eldholm V, Balloux F. 2016. Antimicrobial resistance in *Mycobacterium tuberculosis*: the odd one out. *Trends Microbiol* 24:637–648. <https://doi.org/10.1016/j.tim.2016.03.007>.
- Matsumoto M, Hashizume H, Tomishige T, Kawasaki M, Tsubouchi H, Sasaki H, Shimokawa Y, Komatsu M. 2006. OPC-67683, a nitro-dihydroimidazo[4,5-b]pyridine derivative with promising action against tuberculosis in vitro and in mice. *PLoS Med* 3:e466. <https://doi.org/10.1371/journal.pmed.0030466>.
- Andries K, Verhasselt P, Guillemont J, Gohlmann HW, Neefs JM, Winkler H, Van Gestel J, Timmerman P, Zhu M, Lee E, Williams P, de Chaffoy D, Huitric E, Hoffner S, Cambau E, Truffot-Pernot C, Lounis N, Jarlier V. 2005. A diarylquinoline drug active on the ATP synthase of *Mycobacterium tuberculosis*. *Science* 307:223–227. <https://doi.org/10.1126/science.1106753>.
- Fujiwara M, Kawasaki M, Hariguchi N, Liu Y, Matsumoto M. 2018. Mechanisms of resistance to delamanid, a drug for *Mycobacterium tuberculosis*. *Tuberculosis (Edinb)* 108:186–194. <https://doi.org/10.1016/j.tube.2017.12.006>.
- Huitric E, Verhasselt P, Koul A, Andries K, Hoffner S, Andersson DI. 2010. Rates and mechanisms of resistance development in *Mycobacterium tuberculosis* to a novel diarylquinoline ATP synthase inhibitor. *Antimicrob Agents Chemother* 54:1022–1028. <https://doi.org/10.1128/AAC.01611-09>.
- Fleming A. 1929. On the antibacterial action of cultures of a penicillium, with special reference to their use in the isolation of *B. influenzae*. *Br J Exp Pathol* 10:226–236.
- Newman DJ, Cragg GM. 2012. Natural products as sources of new drugs over the 30 years from 1981 to 2010. *J Nat Prod* 75:311–335. <https://doi.org/10.1021/np200906s>.
- Nwude N, Ibrahim MA. 1980. Plants used in traditional veterinary medical practice in Nigeria. *J Vet Pharmacol Ther* 3:261–273. <https://doi.org/10.1111/j.1365-2885.1980.tb00491.x>.
- Osadebe PO, Omeje EO. 2009. Comparative acute toxicities and immunomodulatory potentials of five Eastern Nigeria mistletoes. *J Ethnopharmacol* 126:287–293. <https://doi.org/10.1016/j.jep.2009.08.024>.
- Oliver-Bever B. 1986. Anti-infective activity of higher plants, p 123–190. *In* Medicinal plants in tropical West Africa. Cambridge University Press, Cambridge, United Kingdom. <https://doi.org/10.1017/CBO9780511753114>.
- Osadebe PO, Ukwueze SE. 2004. A comparative study of the phytochemical and anti-microbial properties of the eastern Nigerian species of African mistletoe (*Loranthus micranthus*) sourced from different host trees. *Bio-Research* 2:18–23. <https://doi.org/10.4314/br.v2i1.28537>.
- Osadebe PO, Akabogu IC. 2006. Antimicrobial activity of *Loranthus micranthus* harvested from kola nut tree. *Fitoterapia* 77:54–56. <https://doi.org/10.1016/j.fitote.2005.08.013>.
- Cemaluk EAC, Nwankwo NE. 2012. Phytochemical properties of some solvent fractions of petroleum ether extract of the African mistletoe (*Loranthus micranthus* Linn) leaves and their antimicrobial activity. *Afr J Biotechnol* 11:12595–12599.
- Ukwueze SE, Osadebe PO, Ezenobi NO. 2013. Bioassay-guided evaluation of the antibacterial activity of *Loranthus* species of the African mistletoe. *Int J Pharm Biomed Res* 4:79–82.
- Hsu FL, Yang LM, Chang SF, Wang LH, Hsu CY, Liu PC, Lin SJ. 2007. Biotransformation of gallic acid by *Beauveria sulfurescens* ATCC 7159. *Appl Microbiol Biotechnol* 74:659–666. <https://doi.org/10.1007/s00253-006-0692-z>.
- Li X, Li Y, Xu W. 2006. Design, synthesis, and evaluation of novel galloyl pyrrolidine derivatives as potential anti-tumor agents. *Bioorg Med Chem* 14:1287–1293. <https://doi.org/10.1016/j.bmc.2005.09.031>.
- Pan S-M, Ding H-Y, Chang W-L, Lin H-C. 2006. Phenols from the aerial parts of *Leonurus sibiricus*. *Chin Pharm J (Taipei, Taiwan)* 58:35–40.
- Savi LA, Leal PC, Vieira TO, Rosso R, Nunes RJ, Yunes RA, Creczynski-Pasa TB, Barardi CRM, Simões CMO. 2005. Evaluation of anti-herpetic and antioxidant activities, and cytotoxic and genotoxic effects of synthetic alkyl-esters of gallic acid. *Arzneimittelforschung* 55:66–75. <https://doi.org/10.1055/s-0031-1296825>.
- Asakawa Y, Matsuda R, Cheminat A. 1987. Bibenzyl derivatives from *Frullania* species. *Phytochemistry* 26:1117–1122. [https://doi.org/10.1016/S0031-9422\(00\)82361-4](https://doi.org/10.1016/S0031-9422(00)82361-4).
- Alam A, Takaguchi Y, Ito H, Yoshida T, Tsuboi S. 2005. Multi-functionalization of gallic acid towards improved synthesis of alpha- and beta-DDB. *Tetrahedron* 61:1909–1918. <https://doi.org/10.1016/j.tet.2004.11.083>.
- Arsianti AA, Astuty H, Fadilah F, Bahtiar A, Tanimoto H, Kakiuchi K. 2017. Design and screening of gallic acid derivatives as inhibitors of malarial dihydrofolate reductase by in silico docking. *Asian J Pharm Clin Res* 10:330–334. <https://doi.org/10.22159/ajpcr.2017.v10i2.15712>.
- Tagashira T, Choshi T, Hibino S, Kamishikiryu J, Sugihara N. 2012. Influence of gallate and pyrogallol moieties on the intestinal absorption of (-)-epicatechin and (-)-epicatechin gallate. *J Food Sci* 77:H208–H215. <https://doi.org/10.1111/j.1750-3841.2012.02902.x>.
- Kim SJ, Myung PK, Sung ND. 2008. CoMFA on the melanogenesis inhibitory activity of alkyl-3,4-dihydroxybenzoate, N-alkyl-3,4-dihydroxybenzamide analogues, and prediction of higher active compounds. *Arch Pharm Res* 31:1540–1546. <https://doi.org/10.1007/s12272-001-2148-4>.
- Kubo I, Fujita K, Nihei K, Nihei A. 2004. Antibacterial activity of alkyl gallates against *Bacillus subtilis*. *J Agric Food Chem* 52:1072–1076. <https://doi.org/10.1021/jf034774l>.
- Kubo I, Xiao P, Fujita K. 2002. Anti-MRSA activity of alkyl gallates. *Bioorg Med Chem Lett* 12:113–116. [https://doi.org/10.1016/S0960-894X\(01\)00663-1](https://doi.org/10.1016/S0960-894X(01)00663-1).
- Silva IC, Regasini LO, Petronio MS, Silva DH, Bolzani VS, Belasque J, Jr, Sacramento LV, Ferreira H. 2013. Antibacterial activity of alkyl gallates against *Xanthomonas citri* subsp. *citri*. *J Bacteriol* 195:85–94. <https://doi.org/10.1128/JB.01442-12>.
- Krol E, de Sousa Borges A, da Silva I, Polaquini CR, Regasini LO, Ferreira H, Scheffers DJ. 2015. Antibacterial activity of alkyl gallates is a combi-

- nation of direct targeting of FtsZ and permeabilization of bacterial membranes. *Front Microbiol* 6:390. <https://doi.org/10.3389/fmicb.2015.00390>.
29. Ioerger TR, Feng YC, Ganesula K, Chen XH, Dobos KM, Fortune S, Jacobs WR, Mizrahi V, Parish T, Rubin E, Sasseti C, Sacchetti JC. 2010. Variation among genome sequences of H37Rv strains of *Mycobacterium tuberculosis* from multiple laboratories. *J Bacteriol* 192:3645–3653. <https://doi.org/10.1128/JB.00166-10>.
 30. Cole ST, Brosch R, Parkhill J, Garnier T, Churcher C, Harris D, Gordon SV, Eiglmeier K, Gas S, Barry CE, III, Tekaiia F, Badcock K, Basham D, Brown D, Chillingworth T, Connor R, Davies R, Devlin K, Feltwell T, Gentles S, Hamlin N, Holroyd S, Hornsby T, Jagels K, Krogh A, McLean J, Moule S, Murphy L, Oliver K, Osborne J, Quail MA, Rajandream MA, Rogers J, Rutter S, Seeger K, Skelton J, Squares R, Squares S, Sulston JE, Taylor K, Whitehead S, Barrell BG. 1998. Deciphering the biology of *Mycobacterium tuberculosis* from the complete genome sequence. *Nature* 393:537–544. <https://doi.org/10.1038/31159>.
 31. Chang Y, Fox BG. 2006. Identification of Rv3230c as the NADPH oxidoreductase of a two-protein DesA3 acyl-CoA desaturase in *Mycobacterium tuberculosis* H37Rv. *Biochemistry* 45:13476–13486. <https://doi.org/10.1021/bi0615285>.
 32. Phetsuksiri B, Jackson M, Scherman H, McNeil M, Besra GS, Baulard AR, Slayden RA, DeBarber AE, Barry CE, III, Baird MS, Crick DC, Brennan PJ. 2003. Unique mechanism of action of the thiourea drug isoxyl on *Mycobacterium tuberculosis*. *J Biol Chem* 278:53123–53130. <https://doi.org/10.1074/jbc.M311209200>.
 33. Grzegorzewicz AE, Kordulakova J, Jones V, Born SE, Belardinelli JM, Vaquie A, Gundi VA, Madacki J, Slama N, Laval F, Vaubourgeix J, Crew RM, Gicquel B, Daffe M, Morbidoni HR, Brennan PJ, Quemard A, McNeil MR, Jackson M. 2012. A common mechanism of inhibition of the *Mycobacterium tuberculosis* mycolic acid biosynthetic pathway by isoxyl and thiacetazone. *J Biol Chem* 287:38434–38441. <https://doi.org/10.1074/jbc.M112.400994>.
 34. Daina A, Michielin O, Zoete V. 2014. iLOGP: a simple, robust, and efficient description of n-octanol/water partition coefficient for drug design using the GB/SA approach. *J Chem Inf Model* 54:3284–3301. <https://doi.org/10.1021/ci5000467k>.
 35. Dyer DH, Lyle KS, Rayment I, Fox BG. 2005. X-ray structure of putative acyl-ACP desaturase DesA2 from *Mycobacterium tuberculosis* H37Rv. *Protein Sci* 14:1508–1517. <https://doi.org/10.1110/ps.041288005>.
 36. Singh A, Varela C, Bhatt K, Veerapen N, Lee OY, Wu HH, Besra GS, Minnikin DE, Fujiwara N, Teramoto K, Bhatt A. 2016. Identification of a desaturase involved in mycolic acid biosynthesis in *Mycobacterium smegmatis*. *PLoS One* 11:e0164253. <https://doi.org/10.1371/journal.pone.0164253>.
 37. Barry CE, III, Lee RE, Mdluli K, Sampson AE, Schroeder BG, Slayden RA, Yuan Y. 1998. Mycolic acids: structure, biosynthesis and physiological functions. *Prog Lipid Res* 37:143–179. [https://doi.org/10.1016/S0163-7827\(98\)00008-3](https://doi.org/10.1016/S0163-7827(98)00008-3).
 38. DeJesus MA, Gerrick ER, Xu W, Park SW, Long JE, Boutte CC, Rubin EJ, Schnappinger D, Ehrt S, Fortune SM, Sasseti CM, Ioerger TR. 2017. Comprehensive essentiality analysis of the *Mycobacterium tuberculosis* Genome via saturating transposon mutagenesis. *mBio* 8:e02133-16. <https://doi.org/10.1128/mBio.02133-16>.
 39. Sasseti CM, Rubin EJ. 2003. Genetic requirements for mycobacterial survival during infection. *Proc Natl Acad Sci U S A* 100:12989–12994. <https://doi.org/10.1073/pnas.2134250100>.
 40. Hao P, Alaraj IQ, Dulayymi JR, Baird MS, Liu J, Liu Q. 2016. Sterculic acid and its analogues are potent inhibitors of *Toxoplasma gondii*. *Korean J Parasitol* 54:139–145. <https://doi.org/10.3347/kjp.2016.54.2.139>.
 41. Li W, Bai H, Liu S, Cao D, Wu H, Shen K, Tai Y, Yang J. 2018. Targeting stearoyl-CoA desaturase 1 to repress endometrial cancer progression. *Oncotarget* 9:12064–12078. <https://doi.org/10.18632/oncotarget.24304>.
 42. Johnstone DB, Little JE. 1953. Bacteriostatic, bactericidal, and drug resistance studies of ethyl gallate on *Mycobacterium tuberculosis*. *J Bacteriol* 66:320–323.
 43. Savietto A, Polaquini CR, Kopacz M, Scheffers DJ, Marques BC, Regasini LO, Ferreira H. 2018. Antibacterial activity of monoacetylated alkyl gallates against *Xanthomonas citri* subsp. *citri*. *Arch Microbiol* <https://doi.org/10.1007/s00203-018-1502-6>.
 44. Takai E, Hirano A, Shiraki K. 2011. Effects of alkyl chain length of gallate on self-association and membrane binding. *J Biochem* 150:165–171. <https://doi.org/10.1093/jb/mvr048>.
 45. Niemann H, Hagenow J, Chung MY, Hellio C, Weber H, Proksch P. 2015. SAR of sponge-inspired hemibastadin congeners inhibiting blue mussel phenoloxidase. *Mar Drugs* 13:3061–3071. <https://doi.org/10.3390/md13053061>.
 46. Rehberg N, Akone HS, Ioerger TR, Erlenkamp G, Daletos G, Gohlke H, Proksch P, Kalscheuer R. 2018. Chlorflavonin targets acetohydroxyacid synthase catalytic subunit IlvB1 for synergistic killing of *Mycobacterium tuberculosis*. *ACS Infect Dis* 4:123–134. <https://doi.org/10.1021/acsinfecdis.7b00055>.
 47. CLSI. 2012. Methods for dilution antimicrobial susceptibility tests for bacteria that grow aerobically. Clinical and Laboratory Standards Institute, Wayne, PA.
 48. Kerry DW, Hamilton-Miller JM, Brumfitt W. 1975. Trimethoprim and rifampicin: in vitro activities separately and in combination. *J Antimicrob Chemother* 1:417–427. <https://doi.org/10.1093/jac/1.4.417>.
 49. Larsen MH, Biermann K, Tandberg S, Hsu T, Jacobs WR, Jr. 2007. Genetic manipulation of *Mycobacterium tuberculosis*. *Curr Protoc Microbiol* Chapter 10:Unit 10A.2. <https://doi.org/10.1002/9780471729259.mc10a02s6>.
 50. Hubatsch I, Ragnarsson EG, Artursson P. 2007. Determination of drug permeability and prediction of drug absorption in Caco-2 monolayers. *Nat Protoc* 2:2111–2119. <https://doi.org/10.1038/nprot.2007.303>.